

Exact solutions for ground effect – supplementary material

Peter. J. Baddoo, Melike. Kurt, Lorna. J. Ayton & Keith W. Moored

This supplementary material includes several details of calculations and methods used in the main paper.

S:1. The prime function $P(\zeta)$

The prime function $P(\zeta)$ was introduced in section 3. Therein, we presented an infinite product representation. Whilst the product form offers physical intuition, it also has poor convergence properties. For numerical computations it is more convenient to express the prime function $P(\zeta)$ as the rapidly convergent Laurent series (Crowdy 2012)

$$P(\zeta) = C \sum_{n=-\infty}^{\infty} (-1)^n q^{n(n-1)} \zeta^n, \quad C = \frac{\prod_{n=1}^{\infty} (1 + q^{2n})^2}{\sum_{n=1}^{\infty} q^{n(n-1)}}. \quad (\text{S:1.1})$$

This series converges quickly except when q is very close to unity. In that case, we recommend calculating the prime function $P(\zeta)$ using the spectral method in Crowdy *et al.* (2016), for which software is freely available (<https://github.com/ACCA-Imperial/SKPrime>).

It is possible to show from the product formula 3.1 that the prime function $P(\zeta)$ has the following properties

$$P(\zeta^{-1}) = -\zeta^{-1}P(\zeta), \quad (\text{S:1.1.a})$$

$$P(q^2\zeta) = -\zeta^{-1}P(\zeta), \quad (\text{S:1.1.b})$$

$$\frac{P(q^2\gamma_1^{-1}\zeta)}{P(q^2\gamma_2^{-1}\zeta)} = \frac{\gamma_1}{\gamma_2} \cdot \frac{P(\gamma_1^{-1}\zeta)}{P(\gamma_2^{-1}\zeta)}. \quad (\text{S:1.1.c})$$

These properties will be used in the derivation of the ground effect conformal maps.

S:2. Derivations of conformal mappings

In this section we derive the conformal mappings presented in section 3.1.

S:2.0.1. Derivation of circular wing map

Given that (3.2) is a Möbius mapping, it maps circlines to circlines. Since $\zeta = 1$ is a simple pole of the mapping, the boundary circle C_0 is mapped to a circle of infinite radius, i.e. a line. It is straightforward to show that this line is the real axis. Additionally, C_1 must be mapped to a circle, and it can be shown that, when $s = 0$, the image of C_1 is centered at $i(q + q^{-1})/4$ and has unit diameter. A typical circular wing map is illustrated in figure S:2.5

S:2.0.2. Derivation of flat plate map

In order to derive the flat plate map (3.3), we will show that f takes constant phase on C_0 and C_1 when the shifting constant s vanishes.

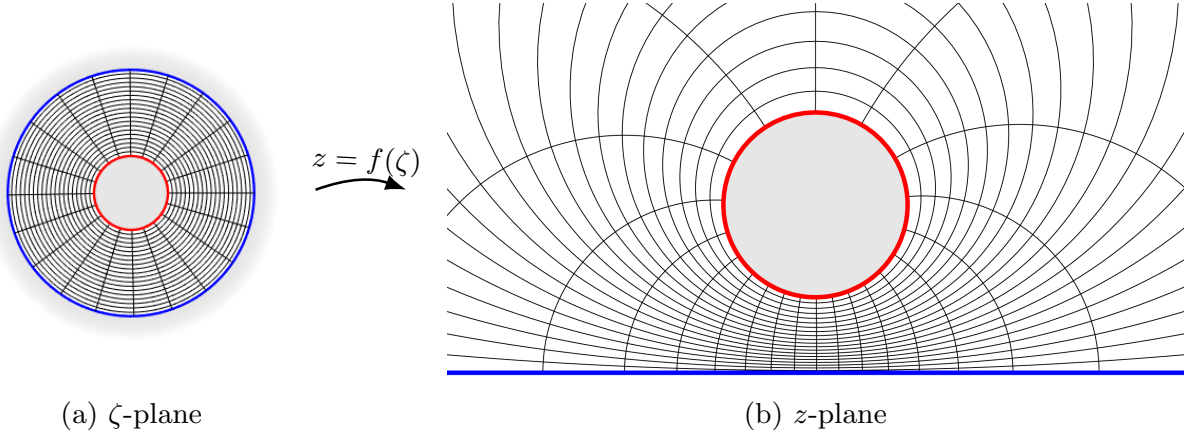


Figure S:2.5: An example of a circular wing map (3.2).

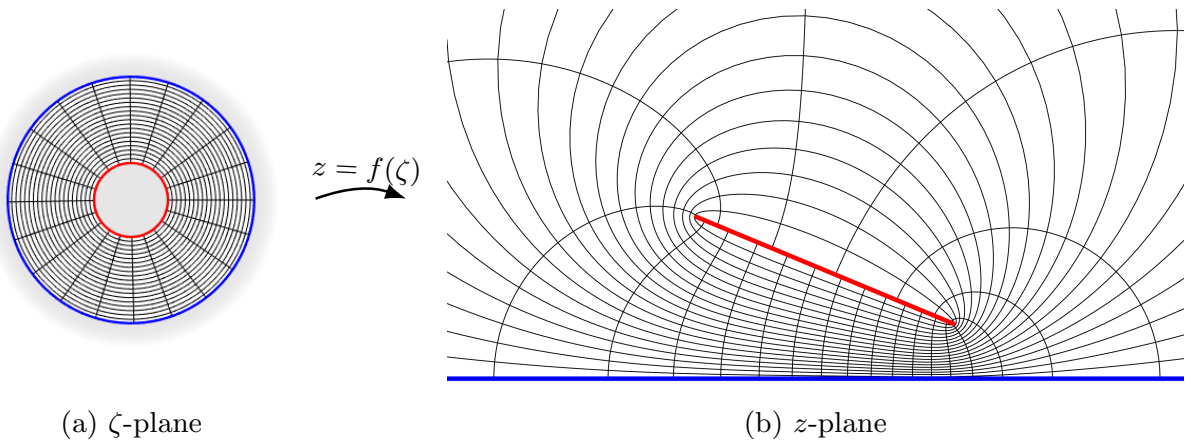


Figure S:2.6: An example of a flat plate wing mapping (3.3).

We write $A = \tilde{A}e^{-i\alpha}$ where $\tilde{A} \in \mathbb{R}$. The complex conjugate of f is then given by

$$\overline{f(\zeta)} = \tilde{A}e^{i\alpha} \frac{P(e^{-2i\alpha}\bar{\zeta})}{P(\bar{\zeta})}. \quad (\text{S:2.1})$$

For $\zeta \in C_0$, we may write $\bar{\zeta} = 1/\zeta$ and use (S:1.1.a) to transform (S:2.1) into

$$\overline{f(\zeta)} = \tilde{A}e^{-i\alpha} \frac{P(e^{2i\alpha}\zeta)}{P(\zeta)} = f(\zeta). \quad (\text{S:2.2})$$

Therefore, f is pure real for $\zeta \in C_0$. Since f contains a simple pole and is univalent, $f(\zeta)$ spans the entire real line.

We now consider the case where $\zeta \in C_1$. In this case, we have $\bar{\zeta} = q^2/\zeta$. Combining this fact with (S:1.1.c) in (S:2.1) yields

$$\overline{f(\zeta)} = \tilde{A}e^{i\alpha} \frac{P(e^{-2i\alpha}/\zeta)}{P(1/\zeta)}. \quad (\text{S:2.3})$$

A further application of (S:1.1.a) yields $\bar{f} = e^{2i\alpha}f$. Therefore, $\arg[f(\zeta)] = -\alpha$ for $\zeta \in C_1$, so f maps C_1 to a slit inclined at an angle of $-\alpha$ to the real axis, which corresponds to a flat plate at angle of attack α .

Typical flat plate wing maps are illustrated in figures S:2.6 and S:2.7.

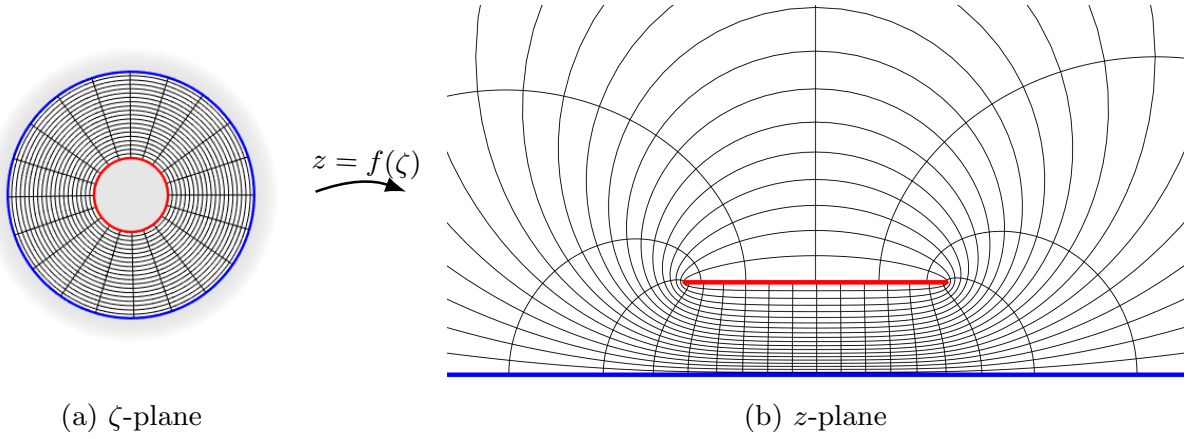


Figure S:2.7: An example of a flat plate wing mapping at zero angle of attack (3.4).

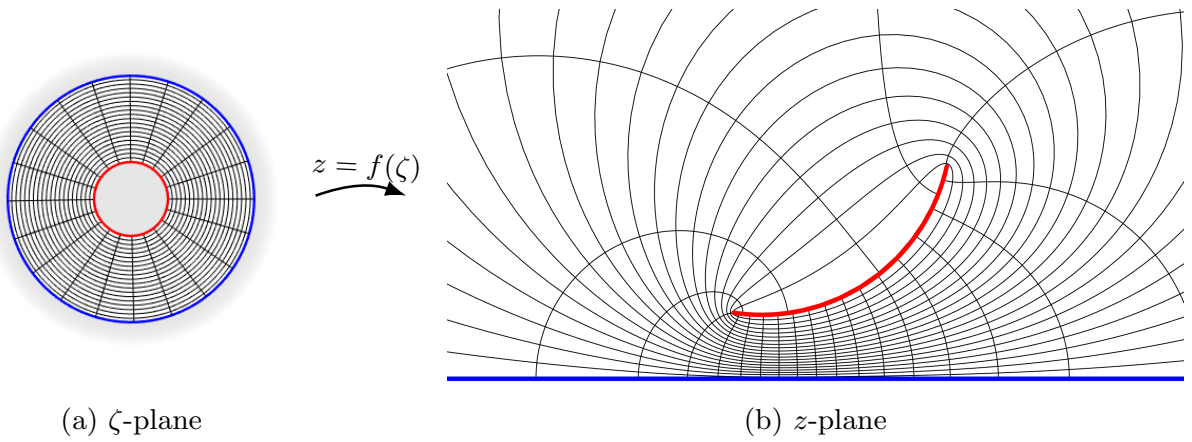


Figure S:2.8: An example of a circular arc wing map (3.5).

S:2.0.3. Derivation of circular arc wing map

We first note that the annulus may be mapped to a circle with a circular arc slit by the mapping (Crowdy & Marshall 2006a)

$$\eta(\zeta, \gamma) = \frac{P(\zeta/\gamma)}{|\gamma|P(\zeta\bar{\gamma})}. \quad (\text{S:2.4})$$

for any $\gamma \in D_\zeta$. This mapping transplants the unit disc onto itself, and C_1 onto a circular arc slit. We now take another Möbius mapping to map the unit circle to the real axis and the circular slit to another circular slit on the upper half plane:

$$f(\zeta) = \frac{B}{\eta(1, \gamma) - \eta(\zeta, \gamma)},$$

where B is a constant required to rotate and scale the map. Note that we have ensured that there is a simple pole at $\zeta = 1$. Composing the mappings gives

$$f(\zeta) = \frac{AP(\zeta\bar{\gamma})}{P(\zeta/\gamma)P(\bar{\gamma}) - P(\zeta/\gamma)P(\zeta\bar{\gamma})},$$

for another constant A .

A typical circular arc wing map is illustrated in figure S:2.8.

S:2.0.4. Derivation of centered circular arc wing map

In order to derive the centered circular arc wing map, we first note that we may write

$$P(\sqrt{\zeta})P(-\sqrt{\zeta}) = P_2(\zeta),$$

where

$$P_2(\zeta) = (1 - \zeta) \prod_{k=1}^{\infty} (1 - q^{4k}\zeta) \cdot (1 - q^{4k}\zeta^{-1}). \quad (\text{S:2.5})$$

The interpretation of P_2 is that it is the prime function $P(\zeta)$ for an annulus where the ratio of exterior to interior radius is q^2 . The analogous forms of (S:1.1.a, S:1.1.b, S:1.1.c) are

$$P_2(\zeta^{-1}) = -\zeta^{-1}P_2(\zeta), \quad (\text{S:2.5.a})$$

$$P_2(q^4\zeta) = -\zeta^{-1}P_2(\zeta), \quad (\text{S:2.5.b})$$

$$\frac{P_2(q^4\gamma_1^{-1}\zeta)}{P_2(q^4\gamma_2^{-1}\zeta)} = \frac{\gamma_1}{\gamma_2} \cdot \frac{P_2(\gamma_1^{-1}\zeta)}{P_2(\gamma_2^{-1}\zeta)}. \quad (\text{S:2.5.c})$$

The centered circular arc wing map (3.6) may therefore be written as

$$f(\zeta) = \tilde{A}e^{-i\phi} \frac{P_2(\zeta e^{2i\phi})P_2(q^2\zeta)}{P_2(q^2\zeta e^{2i\phi})P_2(\zeta)}, \quad (\text{S:2.6})$$

where $A = \tilde{A}e^{-i\phi}$. The first step in the derivation of the circular arc wing map is to see that (S:2.6) is a circular arc slit map on $q < |\zeta| < 1/q$: the circles $|\zeta| = q$ and $|\zeta| = 1/q$ are transplanted to two circular arc slits. We first consider the circle $|\zeta| = q$ so that

$$f(\zeta) = \tilde{A}e^{-i\phi} \frac{P_2(q^4/\bar{\zeta})}{P_2(q^4e^{2i\phi}/\bar{\zeta})} \cdot \frac{P_2(q^2e^{2i\phi}/\bar{\zeta})}{P_2(q^2/\bar{\zeta})},$$

since $\bar{\zeta} = q^2/\zeta$. Application of (S:2.5.c) yields

$$f(\zeta) = \tilde{A}e^{-i\phi} \frac{P_2(1/\bar{\zeta})}{P_2(e^{2i\phi}/\bar{\zeta})} \cdot \frac{P_2(e^{2i\phi}/(q^2\bar{\zeta}))}{P_2(1/(q^2\bar{\zeta}))}.$$

By taking the complex conjugate and applying (S:2.5.a), we see that

$$f(\zeta)\overline{f(\zeta)} = |f(\zeta)|^2 = 1.$$

Therefore the image of $|\zeta| = q$ is a circular arc of unit radius. A similar procedure may be applied to show that the circle $|\zeta| = 1/q$ is also a circular arc.

We now show that the map is anti-symmetric when the argument is reflected in the unit circle. Reflecting the argument of f yields

$$f(1/\bar{\zeta}) = \tilde{A}e^{-i\phi} \frac{P_2(e^{2i\phi}/\bar{\zeta})}{P_2(1/\bar{\zeta})} \cdot \frac{P_2(q^2/\bar{\zeta})}{P_2(q^2e^{2i\phi}/\bar{\zeta})}.$$

Applying (S:2.5.c) to the second fraction gives

$$f(1/\bar{\zeta}) = \tilde{A}e^{i\phi} \frac{P_2(e^{2i\phi}/\bar{\zeta})}{P_2(1/\bar{\zeta})} \cdot \frac{P_2(1/(q^2\bar{\zeta}))}{P_2(e^{2i\phi}/(q^2\bar{\zeta}))}.$$

Now applying (S:2.5.a) to each P_2 yields $f(\zeta) = \overline{f(1/\bar{\zeta})}$. In other words, reflecting the point ζ in the circle $|\zeta| = 1$ results in a reflection of f in the real axis. Since f contains a simple pole at $\zeta = 1$, the unit disc $|\zeta| = 1$ is mapped to the entire real axis.

A typical centered circular arc wing map is illustrated in figure S:2.9.

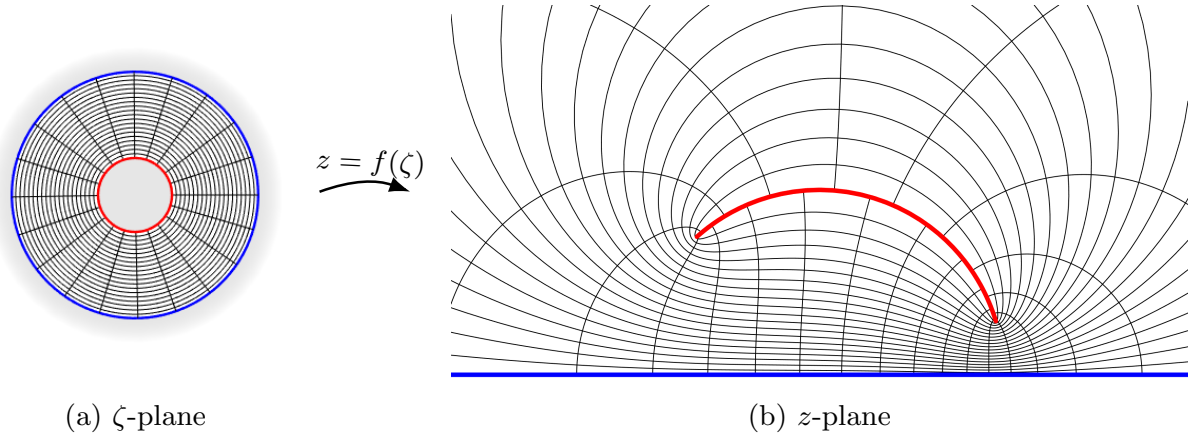


Figure S:2.9: An example of a centered circular arc wing map (3.6).

S:3. Residues of conformal maps

In this section we provide the residues of each conformal map at the simple pole $\zeta = 1$. The residue of the circular wing map (3.2) is

$$a_\infty = \frac{1 - q^2}{i2q}.$$

The residue of the flat plate map (3.3) at angle of attack α is

$$a_\infty = -\frac{AP(e^{2i\alpha})}{L},$$

where $L = \prod_{k=1}^{\infty} (1 - q^{2k})^2$. In the degenerate case where the angle of attack is zero (3.4), the residue is

$$a_\infty = A.$$

The residue for the circular arc wing map (3.5) is

$$a_\infty = \frac{\gamma AP(\bar{\gamma})}{P'(1/\gamma)P(\bar{\gamma}) - |\gamma|^2 P'(\bar{\gamma})P(1/\gamma)}.$$

The residue for the centered circular arc wing map (3.6) is

$$a_\infty = -\frac{2A}{L} \cdot \frac{P(e^{i\phi})P(-e^{i\phi})P(q)P(-q)}{P(qe^{i\phi})P(-qe^{i\phi})P(-1)}.$$

S:4. Derivation of kinematic boundary condition for moving wing

In this section we derive the kinematic boundary condition in the case where the wing executes rigid body motions. We do so by adapting the analysis of Crowdy (2008). Since the ground is stationary, it must represent a streamline. Therefore, the complex potential takes constant imaginary part on C_0 , which we may take to be zero without loss of generality. However, on the wing, the kinematic boundary condition states that fluid on the wing must move at the same velocity as the wing itself:

$$\mathbf{u} \cdot \mathbf{n} = \mathbf{U} \cdot \mathbf{n}, \quad (\text{S:4.1})$$

where \mathbf{u} represents the fluid velocity, \mathbf{n} represents the outward normal direction, and \mathbf{U} represents the velocity of wing. The normal vector \mathbf{n} may be written as $-idz/ds$ where

s is the arc length, so that the kinematic boundary condition (S:4.1) may be written as

$$\operatorname{Re} \left[\bar{u}(s) \times -i \frac{dz}{ds} \right] = \operatorname{Re} \left[\bar{U}(s) \times -i \frac{dz}{ds} \right].$$

In the physical plane, the complex potential due to the motion of the wing is given by w_M . The kinematic condition therefore becomes

$$\operatorname{Re} \left[\frac{dw_M}{dz} \times -i \frac{dz}{ds} \right] = \operatorname{Re} \left[\bar{U}(s) \times -i \frac{dz}{ds} \right]. \quad (\text{S:4.2})$$

The first term may be simplified by the chain rule to

$$\operatorname{Re} \left[-i \frac{dw_M}{ds} \right] = \operatorname{Re} \left[-i \bar{U}(s) \frac{dz}{ds} \right].$$

We now note that the wing may be parametrised as

$$z = id(t) + \xi(s)e^{-i\alpha(t)}.$$

The velocity of the wing may therefore be written as

$$U(s) = i\dot{d}(t) - i\dot{\alpha}(t)\xi(s)e^{-i\alpha(t)} = i\dot{d}(t) - i\dot{\alpha}(t)(z - id(t)),$$

where d represents the (real and positive) distance of the leading edge from the ground, and α represents the angle of attack. The kinematic condition (S:4.2) then becomes

$$\operatorname{Re} \left[-i \frac{dw_M}{ds} \right] = \operatorname{Re} \left[-\dot{d}(t) \frac{dz}{ds} + \dot{\alpha}(t)(\bar{z} - id(t)) \frac{dz}{ds} \right]. \quad (\text{S:4.3})$$

Noting that

$$\frac{d}{ds} |z + id(t)|^2 = 2 \operatorname{Re} \left[(\bar{z} - id(t)) \frac{dz}{ds} \right],$$

we may now integrate the kinematic condition (S:4.3) with respect to s to obtain

$$\operatorname{Re} [-iw_M] = \operatorname{Re} \left[-\dot{d}(t)(z + id(t)) + \frac{\dot{\alpha}(t)}{2} |z + id(t)|^2 \right] + I, \quad (\text{S:4.4})$$

for a constant of integration I which will be chosen to comply with a compatibility condition to be defined later.

We write $W_M(\zeta) = w_M(f(\zeta))$ and translate (S:4.4) into the canonical circular domain to obtain the condition

$$\operatorname{Im} [W_M(\zeta)] = \operatorname{Im} \left[-i\dot{d}(t)(f(\zeta) + id(t)) + i\frac{\dot{\alpha}(t)}{2} |f(\zeta) + id(t)|^2 \right] + I \equiv M(\zeta, \bar{\zeta}), \quad (\text{S:4.5})$$

for $\zeta \in C_1$. Finally, the constant I is given by enforcing a compatibility condition:

$$I = -\frac{1}{2\pi i} \oint_{C_1} \operatorname{Im} \left[-i\dot{d}(t)(f(\zeta') + id(t)) + i\frac{\dot{\alpha}(t)}{2} |f(\zeta') + id(t)|^2 \right] \frac{d\zeta'}{\zeta'}. \quad (\text{S:4.6})$$

Supplementary material references

- CROWDY, D. G. 2008 Explicit solution for the potential flow due to an assembly of stirrers in an inviscid fluid. *J. Eng. Math.* **62** (4), 333–344.
- CROWDY, D. G. 2012 Conformal slit maps in applied mathematics. *ANZIAM J.* **53** (3), 171–189.

- CROWDY, D. G., KROPF, E. H., GREEN, C. C. & NASSER, M. M. S. 2016 The Schottky-Klein prime function: A theoretical and computational tool for applications. *IMA J. Appl. Math.* **81** (3), 589–628.
- CROWDY, D. G. & MARSHALL, J. 2006 Conformal mappings between canonical multiply connected domains. *Comput. Methods Funct. Theory* **6** (1), 59–76.